Base extrusion is found at helical junctions between right- and left-handed forms of DNA and RNA

Doyoun Kim[1], Sanjith Reddy[1], Dong Young Kim[1], Alexander Rich[2], Sangho Lee[3], Kyeong Kyu Kim[1,*] and Yang-Gyun Kim[4,*]

[1]Department of Molecular Cell Biology, Samsung Biomedical Research Institute, Sungkyunkwan University School of Medicine, Suwon 440-746, Korea, [2]Department of Biology, Massachusetts Institute of Technology, Cambridge, MA 02139, USA, Departments of [3]Biological Science and [4]Chemistry, Sungkyunkwan University, Suwon 440-746, Korea

ABSTRACT

Base extrusion is a major structural feature at the junction between B- and Z-DNA (the B–Z junction) where a base pair is broken, and the two bases are extruded from the double helix. Despite the demonstration of base extrusion at the B–Z junction, it is not clear whether a similar base extrusion occurs at other types of junctions involving the left-handed Z conformation. Here, we investigate structural changes of bases at three Z-form junctions: DNA B–Z and Z–Z and RNA A–Z junctions. By monitoring fluorescently labeled duplex nucleic acids using 2-aminopurines at various positions relative to the junction point, we show that base extrusion occurs not only at the DNA B–Z junction, but also at the RNA A–Z and DNA Z–Z junctions. Our data suggest that base extrusion is a general feature of Z-form nucleic-acid junctions.

INTRODUCTION

The study of junction structures formed between helices in nucleic acid has progressed by understanding the structures of Holliday junctions (1,2) and the B-DNA–Z-DNA junctions (3,4). Recent work by Ha *et al.* (3) revealed that base extrusion is a major structural feature at the junction between B-DNA and Z-DNA. At the B–Z junction a base pair is broken, and the two bases are extruded on opposite sides of the double helix. The junction then shows continuous stacking of base pairs between the B-DNA and Z-DNA segments (Figure 1).

There are helical junctions other than the B–Z junction in nucleic-acid duplexes. Very similar left-handed duplexes are formed in both DNA and RNA. Furthermore, the Z conformation has residues that alternate in *syn* and *anti* conformations. When this duplex repeat is disrupted, it creates a Z–Z junction (5–7). The Z–Z junction marks the boundary between two out-of-phase Z-DNA regions (6). In addition, the RNA duplex can have an A–Z junction when Z-form RNA is formed. The detailed crystal structure of the B–Z junction was revealed in our previous study (3); however, the structural features of B–Z, Z–Z and A–Z junctions in solution are still to be investigated.

Formation of Z-DNA under physiological conditions has remained a major experimental challenge for investigating Z-form-containing helical junctions of DNA and RNA. The use of a protein Z-DNA-binding domain (Zα of human ADAR1) made it possible to determine the crystal structure of B–Z junction (3). In that study, the double-stranded RNA adenosine deaminase (ADAR1) Zα domain readily stabilized Z-DNA under physiological condition, while the DNA segment with an unfavorable sequence for Z-DNA formation remained in the B-conformation. Likewise, Zα can convert an RNA duplex composed of r(CG) repeats into Z-form RNA (8). When salt is used to stabilize Z-RNA, it requires a higher salt concentration and temperature than is needed for DNA (9,10). Thus, Zα is shown to be a powerful tool to stabilize Z-RNA under physiological conditions.

Nucleotide bases can also be removed from the stacked bases at the center of nucleic-acid duplexes by a variety of base modifying enzymes. That process is generally referred to as 'base flipping' in that the enzyme actively promotes removal of the base from the stacked bases. However, *in vivo*, the bases at the B–Z junction are not actively removed from the stacked bases by an external agent, but are rather forced out by torsional strain of the duplex. Thus, we use the term 'base extrusion' rather than 'base flipping'.

2-Aminopurine (2AP) is a fluorescent base analog of adenine, and it can be incorporated in DNA with little effect on its structure (11) and function (12,13).

*To whom correspondence should be addressed. Email: kkim@med.skku.ac.kr
Correspondence may also be addressed to Yang-Gyun Kim. Tel: +82 31 299 4563; Fax: +82 31 299 4575; Email: ygkimmit@skku.edu; ygkimmit@gmail.com
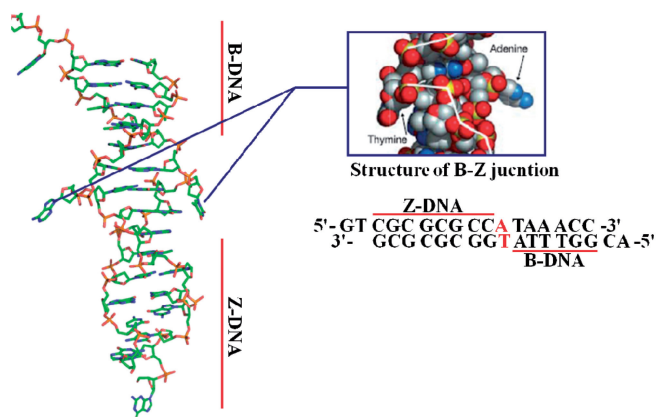
Figure 1. Crystal structure of the B–Z junction. Extruded bases at the junction are colored in red in the sequences. The conformations of the DNA regions are indicated by a red line and bold letters. [The figure is reconstructed from PDB ID:2ACJ].

In addition, 2AP has strong fluorescence compared to the natural bases (14). 2AP fluorescence is significantly quenched in duplex nucleic acids due to stacking interactions with neighboring bases. When a 2AP is extruded from the duplex, its fluorescence considerably increases. Thus, it is an ideal probe to investigate junctions with Z-form nucleic-acid duplexes. 2AP has been used frequently for detecting dynamic structural changes of bases in DNA (11,15–17), as well as in base flipping of the targeted base by N6 adenine DNA methyltransferase and *EcoR*I DNA methyltransferase (18–20).

Here, we ask whether base extrusion is a general structural feature for various Z-form-containing junctions by exploring base extrusion in three types of Z-form-containing junctions: B–Z, A–Z and Z–Z junctions. The fluorescence of 2APs distinguishes between stacked bases and unstacked bases. We show that base extrusion is a common feature of junctions between opposite helical handednesses of double-stranded nucleic acids.

MATERIALS AND METHODS

Preparation of duplex oligonucleotides

2-aminopurine (2AP) modified and unmodified single-stranded oligonucleotides (Table 1) were purchased from Integrated DNA Technologies (IDT, San Diego, CA, USA). All oligonucleotides were equilibrated against buffer containing 50 mM Tris–HCl, pH 8.0, 50 mM NaCl and 1 mM EDTA. Equimolar amounts of complementary sequences were mixed together and annealed. After annealing, the duplex oligonucleotides were purified by using a MonoQ column (Amersham Biosciences). Purified duplex oligonucleotides were dialyzed against buffer containing 5 mM HEPES, pH 7.5 and 10 mM NaCl. The concentration of the duplex DNA was calculated using UV quantification.

Expression and purification of protein

The gene coding for the Zα domain (140–202) of human ADAR1 (Zα) was subcloned into pET28a (Novagen) and transformed into BL21(DE3). The cells were grown in LB containing 30 μg/ml kanamycin to an OD_{600} of 0.5–0.6 at 37°C, and then induced with 0.5 mM isopropyl β-D-thiogalactoside (IPTG) at 37°C for 4 h. Zα was purified using methods described previously (21). After a His-affinity column (Amersham Bioscience) and removal of the N-terminal six histidines with thrombin (Boehringer Mannheim), the protein in buffer A (20 mM HEPES, pH 7.5 and 10 mM NaCl) was further purified using Resource S (Amersham Biosciences). The purified protein was dialyzed against buffer containing 5 mM HEPES, pH 7.5 and 10 mM NaCl. After dialysis, the protein was concentrated to over 1 mM by ultrafiltration on a Centricon-YM3 device (Millipore). All of the buffer change steps were carried out using molecular porous membrane tubing (Spectrum laboratories, Inc). The protein concentration was measured spectroscopically using an extinction coefficient of $6970 \, M^{-1}cm^{-1}$ at 280 nm, calculated at www.expasy.org.

Circular dichroism

The conversion of duplex oligonucleotides (Table 1) from B-DNA to Z-DNA was monitored by measuring the circular dichroism (CD) spectrum using a Jasco J-810 CD spectrometer at 25°C with 15 μM of dsDNA (BZ0, BZ1, BZ4 and ZZ substrates). Z-RNA measurements used 7.5 μM of dsRNA (AZ0, AZ1 or AZ4). All solutions were in buffer containing 10 mM HEPES–NaOH, pH 7.5, 10 mM NaCl. Zα was added to dsDNA solution to a final concentration of 15 μM (1×), 30 μM (2×), 45 μM (3×), 60 μM (4×) and 75 μM (5×) Zα was added to the RNA solution to a final concentration of 7.5 μM (1×), 15 μM (2×), 22.5 μM (3×), 30 μM (4×) and 37.5 μM (5×). The mixtures were equilibrated for 1 h for dsDNA and 2 h for dsRNA prior to the measurement. Spectra were recorded between 230 nm to 320 nm at 1 nm intervals averaged over 2 s. The maximum volume of the protein added to the sample did not exceed 5% of the total volume.

Steady-state fluorescence

Fluorescence measurements were carried out at 25°C using a Quartz Fluorometer Cell Microsquare 3 mm (Starna Cells, Inc., Atascadero, CA, USA). Titrations of duplex oligonucleotides in buffer, which contains 20 mM HEPES–NaOH (pH 7.5) at each concentration of Zα, were performed to reach equilibrium as monitored by the CD spectrum in which the wavelength was fixed at 255 nm and 280 nm, respectively (Data not shown). Fluorescence intensities of deoxyoligonucleotides— 15 μM of dsDNA (BZ0, BZ1, BZ4 and ZZ substrates) and 7.5 μM of dsRNA (AZ0, AZ1 and AZ4 substrates) were measured with increasing Zα concentrations. Duplex oligonucleotides were excited at 320 nm and emission data were collected between 335 nm and 500 nm.

Fluorescence data analysis

All fluorescence emission spectra and fluorescence intensities from titrations were corrected by subtracting the control buffer spectra. Because the 2-aminopurine

fluorescence is highly affected by their position relative to adenines in the oligonucleotide (22), fluorescence emission spectra were corrected by subtracting the control spectra containing buffer only.

RESULTS

Base extrusion at the B–Z junction

Oligonucleotide DNA and RNA duplexes were synthesized with sequences that were somewhat related to the sequence of the B–Z junction which was crystallized (4). One end of the molecule had (CG) repeats that readily form left-handed Z structures, while the other end had sequences that resisted Z formation. Various positions containing adenine near the expected junction were substituted with 2AP. The experimental design consists of measuring fluorescence in the various samples as the concentration of the Z-binding protein increases, starting from zero. When the 2AP is in a base pair with thymine (or uracils), the fluorescence will be only slightly perturbed as the Z-binding protein is added. However, if the 2AP base pair is broken and 2AP is extruded, there will be a significant increase in fluorescence. In the case of the ZZ oligonucleotide, the alternations of d(CG) is disrupted by a single 2AP:thymine base pair, and the fluorescence is visualized directly as the Z-binding protein is added.

The 2AP-modified oligonucleotides are shown in Table 1. 2APs were inserted at three different positions in BZ oligonucleotides, BZ0, BZ1 and BZ4 (Table 1), respectively. The transition from all B- to half Z-DNA conformation in synthesized oligonucleotides was induced by adding purified Z-binding protein, Zα and monitored by CD. The CD data confirmed that all three BZ duplexes were able to form Z-DNA, as induced by the Zα protein in the region containing the d(CG) repeats (Supplementary Figure S1). The saturation of Z-DNA formation occurred approximately at a ratio of 4:1 (Protein:dsDNA) for all three BZ substrates.

The fluorescence change from the BZ0 duplex illustrates the behavior of the 2AP:T base-pairing at a canonical B–Z junction, based on the previous crystal structure (3). On the other hand, 2APs in BZ1 and BZ4 duplexes are located one- and four-nucleotide away from the B–Z junction, respectively. Steady-state fluorescence measurements were used to demonstrate base extrusion at the potential helical junctions. Fluorescence emission spectra of BZ0 showed that extensive changes occurred to the 2AP during the B-to-Z transition induced by Zα (Figure 2A). When fluorescence changes are plotted as a function of the Zα/dsDNA ratio, a large increase is seen in the fluorescence signal at 380 nm in BZ0 consistent with base extrusion of the 2AP as the B-to-Z-DNA conversion takes place with added Zα protein (Figure 2D). The fluorescence spectrum change of BZ0 shows a saturation at a Zα/dsDNA ratio of 4:1 (Figure 2D). This result indicates that base extrusion is coupled to Z-DNA formation.

These results suggest that the 2AP base-paired with the complementary T of BZ0 is undergoing breakage of the pairing and extrusion out of the double helix to form the B–Z junction. In contrast, the 2APs of either BZ1 or

**Table 1.** Sequences of duplex oligonucleotides and their abbreviations used in this study

Abbreviation	Sequence
BZ0	5′-CGCGCGCGCGCG**A**TAAACCACTCGG-3′
	3′-GCGCGCGCGCGC**T̄**ATTTGGTGAGCC-5′
BZ1	5′-CGCGCGCGCGCGAT**A**AACCACTCGG-3′
	3′-GCGCGCGCGCGCT**A**TTTGGTGAGCC-5′
BZ4	5′-CGCGCGCGCGCGA**T**AAACCACTCGG-3′
	3′-GCGCGCGCGCGCTATT**T̄**GGTGAGCC-5′
AZ0	5′-CGCGCGCGCGCG**A**UAAACCACUCGG-3′
	3′-GCGCGCGCGCGC**Ū**AUUUGGUGAGCC-5′
AZ1	5′-CGCGCGCGCGCGAU**A**AACCACUCGG-3′
	3′-GCGCGCGCGCGCU**A**UUUGGUGAGCC-5′
AZ4	5′-CGCGCGCGCGCGA**Ū**AAACCACUCGG-3′
	3′-GCGCGCGCGCGCUAUU**Ū**GGUGAGCC-5′
ZZ	5′-CGCGCGCGTCGCGCGCG-3′
	3′-GCGCGCGC**A̱**GCGCGCGC-3′

The modified base 2-amino-purine is printed in bold and underlined. The AZ-series oligonucleotides are all ribonucleic acids. The BZ series and ZZ are all deoxyribonucleic acids.

BZ4 showed much less prominent fluorescence spectrum changes (Figure 2B and C), indicating a minimal base extrusion and little effect on stacking interactions. The most probable explanation would be that the local changes experienced by the 2APs in BZ1 and BZ4 associated with Z-DNA formation were significantly smaller compared to those seen in BZ0. It is likely that these minimal changes are due to perturbations in base-stacking interactions in the remaining B-DNA region of both BZ1 and BZ4. These results from BZ duplexes are fully consistent with the crystal structure of the B–Z junction, which maintains normal base stacking (3).

Base extrusion at an RNA A–Z junction

Double-stranded RNA is known to adopt the A-conformation which differs considerably from the DNA B-conformation. However, double-stranded RNA composed of r(CG) repeats can be converted into the Z conformation in the presence of Zα (8). The crystal structure of Z-RNA, when complexed to Zα, is very similar to Z-DNA (23). In the presence of Zα protein, an A–Z junction can be formed using a substrate containing r(CG) repeats at one end and a non-Z-potentiating sequence at the other end. The designed double-stranded RNA substrates (AZ0, AZ1 and AZ4) used for investigating A–Z junctions contain the same nucleotide sequences as used in the BZ-series DNA substrates, except uracils replace thymines (Table 1). As anticipated, CD data demonstrated that the A-to-Z transition occurs in AZ0, AZ1 and AZ4 when Zα is added to the solution (Supplementary Figure S2). The fluorescence spectrum changes of 2APs in the AZ substrates were then monitored. The 2AP positioned at the anticipated A–Z junction base pair of the AZ0 experienced a large fluorescence spectrum change on addition of Zα, which implies that base extrusion of the 2AP occurs as Z-RNA is formed, similar to that of BZ0 (Figure 3A). Comparison of fluorescence change of AZ1 with that of AZ4 revealed that AZ1 showed larger fluorescence changes, unlike AZ4 (Figure 3B, C and D).
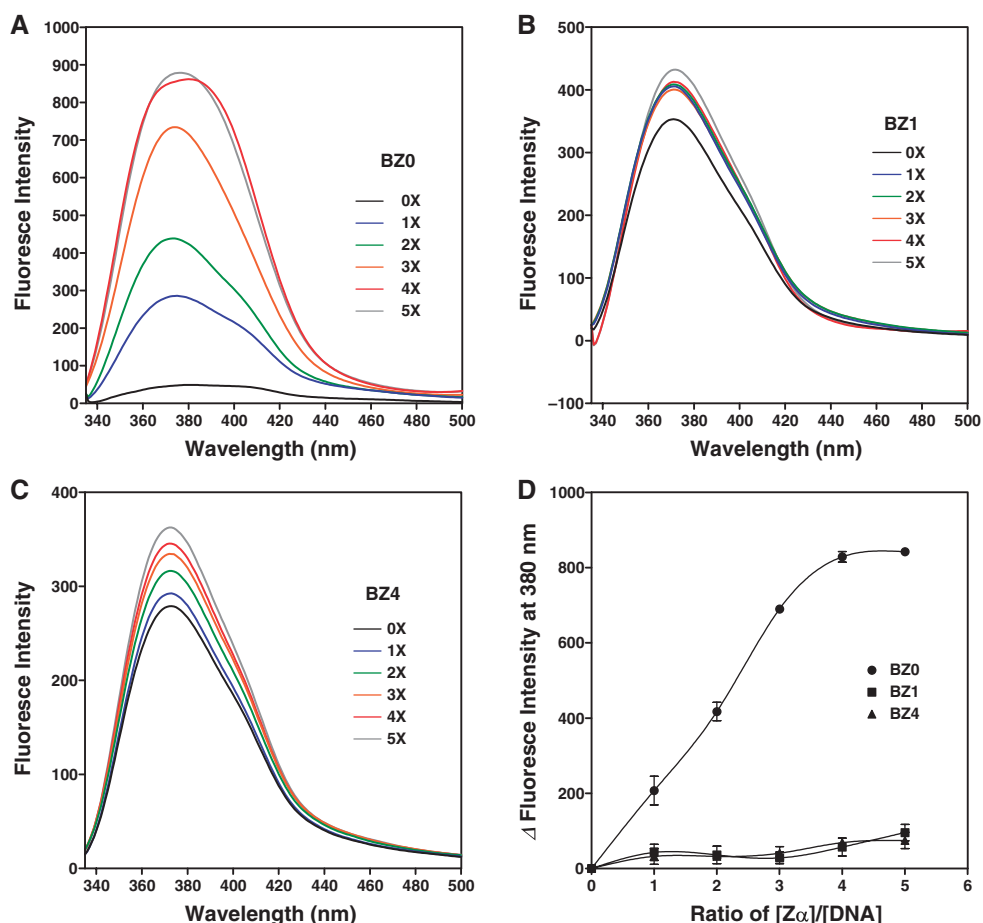
Figure 2. Fluorescence emission profile and B–Z junction-dependent intensity changes as a function of Zα concentration. (**A–C**) Steady-state fluorescence emission intensities in the BZ-series of DNA substrates were taken after 30 min incubation with Zα protein at each molar ratio of protein:DNA (0× to 5×). Samples containing 15 μM duplex DNA were excited at 320 nm and emission spectra were scanned between 335 nm and 500 nm. (**D**) Intensity changes of fluoresce emission at 380 nm were compared at different Zα concentration—0× = no protein; 1× = 15 μM; 2× = 30 μM; 3× = 45 μM; 4× = 60 μM; 5× = 75 μM. In the absence of Zα, intensity at 380 nm in arbitrary units was defined as 0 (I_0) and each of the following intensity changes were calculated by subtracting I_0 from the intensity at 380 nm at different protein concentrations.

Thus, AZ1 seems to show a slight Zα-dependent increase of emission signal at 380 nm (Figure 3D). In comparison, AZ4 showed virtually no increase in the fluorescence signal. This observation suggests an altered base pair stacking at the A–Z junction, compared to that observed in the B–Z junction structure (3). However, at this stage, the evidence is suggestive, but not definitive to conclusively support an extruded base at the A–Z junction. Further experimental work such as chemical probing and structural determination will be needed in order to demonstrate it conclusively.

Base extrusion at a Z–Z junction

Our final investigation concerned the structural changes at a Z–Z junction. In the ZZ substrate, two d(CG)$_4$ regions are separated by a single 2AP:T base-pair which brings the two d(CG) regions out-of-phase with each other. Both sides of the ZZ duplex can form Z-DNA stabilized by Zα binding. As a result, the region at the 2-AP:T base-pair will create a Z–Z junction. The CD results showed that Zα proteins binding to the ZZ duplex results in a high degree of Z-DNA formation, detected by an almost complete conversion of B-DNA to Z-DNA seen in the CD spectrum (Supplementary Figure S3). However, Z-DNA formation should not be continuous throughout the whole ZZ duplex because the two alternating pyrimidine/purine repeats are out-of-phase due to the 2AP:T base-pair in the middle. Accordingly, a Z–Z junction is anticipated to form near the 2AP:T base pair with extrusion to allow continuous Z-DNA formation. As shown in Figure 4, the fluorescence spectrum change of the 2AP in the ZZ substrate is dependent on the addition of Zα protein and Z-DNA formation. This shows that the formation of the Z–Z junction involves significant topological changes in the 2AP base at the junction region consistent with a probable base extrusion upon Z-DNA formation.

DISCUSSION

Base extrusion may provide a general mechanism for relieving strain conferred on Z-form double helices
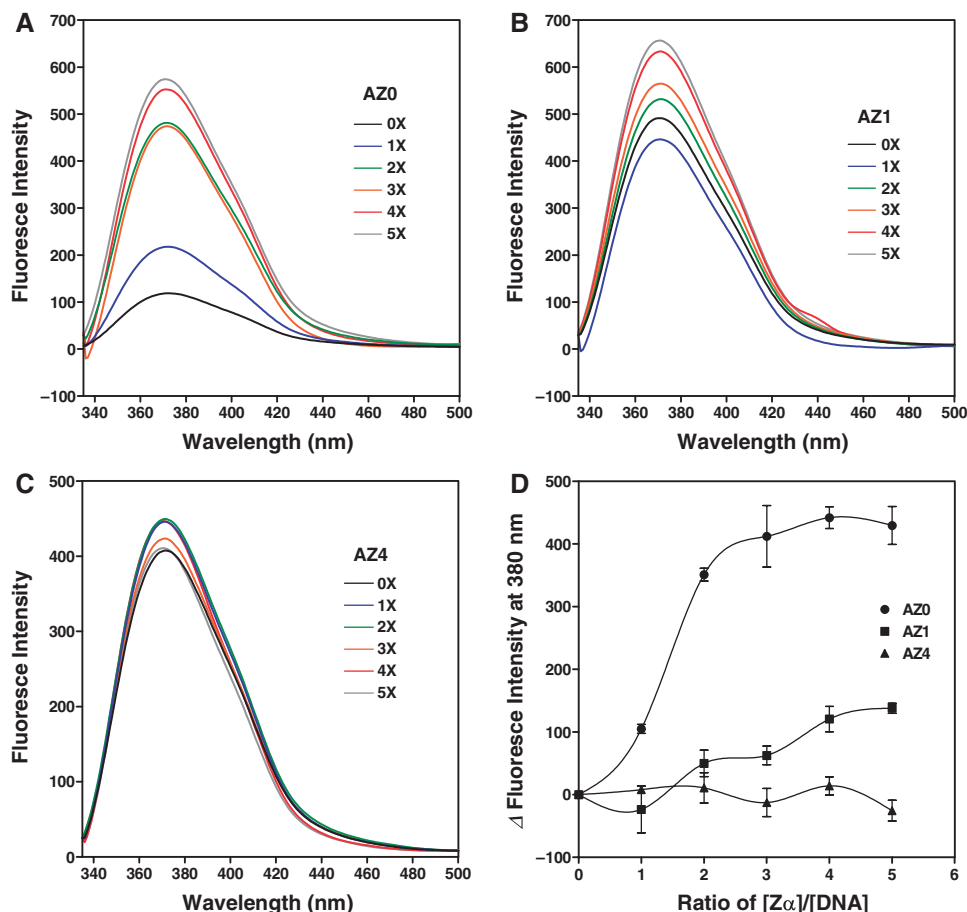
Figure 3. Fluorescence emission profile and A–Z junction-dependent intensity changes as a function of Zα concentration. (**A–C**) Steady-state fluorescence emission intensities of the AZ-series of RNA substrates, AZ0, AZ1 and AZ4, were taken after 2 h incubation with Zα protein at each molar ratio of protein:RNA (0× to 5×). Samples containing 7.5 μM duplex RNA were excited at 320 nm and emission spectra were scanned between 335 nm and 500 nm. (**D**) Intensity changes of fluoresce emission at 380 nm were compared at different Zα concentration—0× = no protein; 1× = 7.5 μM; 2× = 15 μM; 3× = 22.5 μM; 4× = 30 μM; 5× = 37.5 μM. In the absence of Zα, intensity at 380 nm in arbitrary units was defined as 0 (I_0) and each following intensity changes were calculated by subtracting I_0 from an intensity at 380 nm at different protein concentrations.
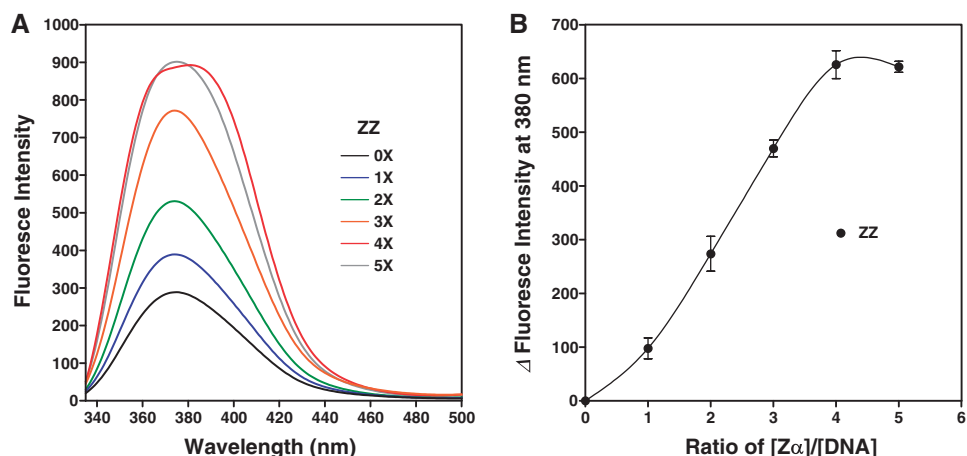
Figure 4. Fluorescence emission profile and Z–Z junction-dependent intensity changes as a function of Zα concentration. (**A**) Samples containing 15 μM duplex DNA were excited at 320 nm and emission spectra were scanned between 335 nm and 500 nm. (**B**) Intensity changes in fluoresce emission at 380 nm were compared at different Zα concentration—0× = no protein; 1× = 15 μM; 2× = 30 μM; 3× = 45 μM; 4× = 60 μM; 5× = 75 μM. In the absence of Zα, intensity at 380 nm in arbitrary units was defined as 0 (I_0), and each of the following intensity changes were calculated by subtracting I_0 from the intensity at 380 nm at different protein concentrations.
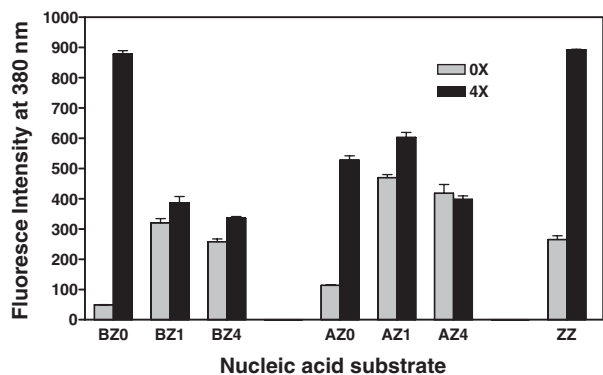
Figure 5. Comparison of fluorescence intensity at different 2-AP positions with and without Zα. Fluorescence intensity of substrates containing no Zα protein (0×, grey bars) was compared with that in the presence of a 4-fold excess of Zα over nucleic-acid substrates (4×, solid bars). Intensity numbers were taken from fluorescence intensities at 380 nm for each nucleic-acid substrate. All measurements were repeated three times and results were averaged.

during junction formation. A local melting of the double helix is probably a prerequisite for reorganizing the handedness of helices involving unpairings and pairings of complementary bases from opposite strands. During junction formation, double helical nucleic acids must undergo a drastic change to avoid topological constraints imposed by formation of the left-handed duplex. One of the base-pairings remains unpaired to form a junction structure. As shown in Figure 5, the inserted 2AP bases (BZ0, AZ0 and ZZ) that are located near the potential junction region generate significant increases of fluorescence emission signals in a Z-form-dependent manner while the 2-APs distant from the junctions (BZ1, BZ4, AZ1 and AZ4) showed almost none or little changes (Figure 5). Our results indicate that Z-form-containing junctions share a common structural feature; base extrusion is likely to be induced at the junctions, consistent with the crystal structure of the B–Z junction. Like the B–Z junction, the A–Z and Z–Z junctions have fluorescence changes consistent with base extrusion. Although no structural data is yet available for the A–Z junction, base extrusion at the Z–Z junction is in good agreement with the chemical modification study, which showed that the Z–Z junction is limited to 1–2 base-pairs and costs less energetically than a B–Z junction (6). Due to base extrusion, the surrounding junctions do not suffer significant destabilization of base-pairing or base stacking. Thus, this minimizes the energy cost of forming a junction.

There appear to be slight differences among the junctions. Unlike the B–Z junction, our results suggest that a nearby base-pair containing a 2AP in the A–Z junction (AZ1, Figures 3D and 5) underwent small but noticeable changes in fluorescence signals compared to that of AZ4. A–Z junction may have different stacking interactions around the junction due to the partial melting of the base-pairing next to the junctional base-pair or a defective base stacking between the A-RNA and Z-RNA regions. It is thought that B-DNA is generally more flexible than RNA. In some cases, however, A-RNA can be easier to

deform (24). In addition, continuous base stacking through the B–Z junction may be more favorable than that at an A–Z junction. The dissimilarity of the base-stacking environment is larger between A-RNA and Z-RNA. A-RNA has a greater diameter than Z-RNA. Furthermore, the base pair tilt relative to the helical axis in A-RNA is not found in Z-RNA, leading to a short kink at the junction. This could result in somewhat loose or incomplete stacking interactions near the A–Z junction.

Our results shed light on possible relations between base extrusion that occurs at the junctions described above and their biological roles. There are some structural similarities between the extruded bases at the Z-type junctions and the bases that are flipped due to base-modifying enzyme/substrate complexes (25–27). It is possible that the extruded Z-type junctional bases might be targets for base-modification under some conditions. In addition, the altered nucleic-acid backbone around these junctions can be sensitive to structure-specific nucleases. Wang *et al.* (28) suggested that Z-DNA-forming sequences induce double-strand breaks nearby, resulting in large-scale deletions in a non-sequence-specific manner. It is tempting to suggest involvement of structure-specific nucleases or other protein factors that recognize structural features created by junction formation such as B–Z, A–Z and Z–Z junctions, as suggested in other work (3,5,6).

Base extrusion as the unique intrinsic feature of these junctions can serve as a signature for structural changes in these nucleic acids. A 2AP undergoing base extrusion could be utilized as a highly sensitive biosensor responding to changing environments such as temperature (16,17). In addition, understanding of junction structures occurring in double helical nucleic acids would greatly assist our understanding of the roles of these versatile junctions that reverse handedness of double helices.

SUPPLEMENTARY DATA

Supplementary Data are available at NAR Online.

FUNDING

Conflict of interest statement. None declared.

REFERENCES

1. Biertumpfel,C., Yang,W. and Suck,D. (2007) Crystal structure of T4 endonuclease VII resolving a Holliday junction. *Nature*, **449**, 616–620.

2. Hadden,J.M., Declais,A.C., Carr,S.B., Lilley,D.M. and Phillips,S.E. (2007) The structural basis of Holliday junction resolution by T7 endonuclease I. *Nature*, **449**, 621–624.

3. Ha,S.C., Lowenhaupt,K., Rich,A., Kim,Y.G. and Kim,K.K. (2005) Crystal structure of a junction between B-DNA and Z-DNA reveals two extruded bases. *Nature*, **437**, 1183–1186.

4. Sheardy,R.D., Levine,N., Marotta,S., Suh,D. and Chaires,J.B. (1994) A thermodynamic investigation of the melting of B-Z junction forming DNA oligomers. *Biochemistry*, **33**, 1385–1391.

5. McLean,M.J., Lee,J.W. and Wells,R.D. (1988) Characteristics of Z-DNA helices formed by imperfect (purine-pyrimidine) sequences in plasmids. *J. Biol. Chem.*, **263**, 7378–7385.

6. Johnston,B.H., Quigley,G.J., Ellison,M.J. and Rich,A. (1991) The Z-Z junction: the boundary between two out-of-phase Z-DNA regions. *Biochemistry*, **30**, 5257–5263.

7. Johnston,B.H. and Rich,A. (1985) Chemical probes of DNA conformation: detection of Z-DNA at nucleotide resolution. *Cell*, **42**, 713–724.

8. Brown,B.A. 2nd, Lowenhaupt,K., Wilbert,C.M., Hanlon,E.B. and Rich,A. (2000) The zalpha domain of the editing enzyme dsRNA adenosine deaminase binds left-handed Z-RNA as well as Z-DNA. *Proc. Natl Acad. Sci. USA*, **97**, 13532–13536.

9. Hall,K., Cruz,P., Tinoco,I. Jr., Jovin,T.M. and van de Sande,J.H. (1984) 'Z-RNA'–a left-handed RNA double helix. *Nature*, **311**, 584–586.

10. Klump,H.H. and Jovin,T.M. (1987) Formation of a left-handed RNA double helix: energetics of the A-Z transition of poly[r(G-C)] in concentrated NaClO4 solutions. *Biochemistry*, **26**, 5186–5190.

11. Larsen,O.F., van Stokkum,I.H., Gobets,B., van Grondelle,R. and van Amerongen,H. (2001) Probing the structure and dynamics of a DNA hairpin by ultrafast quenching and fluorescence depolarization. *Biophys. J.*, **81**, 1115–1126.

12. Raney,K.D., Sowers,L.C., Millar,D.P. and Benkovic,S.J. (1994) A fluorescence-based assay for monitoring helicase activity. *Proc. Natl Acad. Sci. USA*, **91**, 6644–6648.

13. Ujvari,A. and Martin,C.T. (1996) Thermodynamic and kinetic measurements of promoter binding by T7 RNA polymerase. *Biochemistry*, **35**, 14574–14582.

14. Ward,D.C., Reich,E. and Stryer,L. (1969) Fluorescence studies of nucleotides and polynucleotides. I. Formycin, 2-aminopurine riboside, 2,6-diaminopurine riboside, and their derivatives. *J. Biol. Chem.*, **244**, 1228–1237.

15. Kelley,S.O., Boon,E.M., Barton,J.K., Jackson,N.M. and Hill,M.G. (1999) Single-base mismatch detection based on charge transduction through DNA. *Nucleic Acids Res.*, **27**, 4830–4837.

16. Tashiro,R. and Sugiyama,H. (2003) A nanothermometer based on the different pi stackings of B- and Z-DNA. *Angew. Chem. Int. Ed Engl.*, **42**, 6018–6020.

17. Tashiro,R. and Sugiyama,H. (2005) Biomolecule-based switching devices that respond inversely to thermal stimuli. *J. Am. Chem. Soc.*, **127**, 2094–2097.

18. Allan,B.W. and Reich,N.O. (1996) Targeted base stacking disruption by the EcoRI DNA methyltransferase. *Biochemistry*, **35**, 14757–14762.

19. Holz,B., Klimasauskas,S., Serva,S. and Weinhold,E. (1998) 2-Aminopurine as a fluorescent probe for DNA base flipping by methyltransferases. *Nucleic Acids Res.*, **26**, 1076–1083.

20. Allan,B.W., Reich,N.O. and Beechem,J.M. (1999) Measurement of the absolute temporal coupling between DNA binding and base flipping. *Biochemistry*, **38**, 5308–5314.

21. Schwartz,T., Rould,M.A., Lowenhaupt,K., Herbert,A. and Rich,A. (1999) Crystal structure of the Zalpha domain of the human editing enzyme ADAR1 bound to left-handed Z-DNA. *Science*, **284**, 1841–1845.

22. Davis,S.P., Matsumura,M., Williams,A. and Nordlund,T.M. (2003) Position dependence of 2-aminopurine spectra in adenosine pentadeoxynucleotides. *J. Fluoresc.*, **13**, 249–259.

23. Placido,D., Brown,B.A. 2nd, Lowenhaupt,K., Rich,A. and Athanasiadis,A. (2007) A left-handed RNA double helix bound by the Z alpha domain of the RNA-editing enzyme ADAR1. *Structure*, **15**, 395–404.

24. Perez,A., Noy,A., Lankas,F., Luque,F.J. and Orozco,M. (2004) The relative flexibility of B-DNA and A-RNA duplexes: database analysis. *Nucleic Acids Res.*, **32**, 6144–6151.

25. Klimasauskas,S., Kumar,S., Roberts,R.J. and Cheng,X. (1994) HhaI methyltransferase flips its target base out of the DNA helix. *Cell*, **76**, 357–369.

26. Daniels,D.S., Woo,T.T., Luu,K.X., Noll,D.M., Clarke,N.D., Pegg,A.E. and Tainer,J.A. (2004) DNA binding and nucleotide flipping by the human DNA repair protein AGT. *Nat. Struct. Mol. Biol.*, **11**, 714–720.

27. Vassylyev,D.G., Kashiwagi,T., Mikami,Y., Ariyoshi,M., Iwai,S., Ohtsuka,E. and Morikawa,K. (1995) Atomic model of a pyrimidine dimer excision repair enzyme complexed with a DNA substrate: structural basis for damaged DNA recognition. *Cell*, **83**, 773–782.

28. Wang,G., Christensen,L.A. and Vasquez,K.M. (2006) Z-DNA-forming sequences generate large-scale deletions in mammalian cells. *Proc. Natl Acad. Sci. USA*, **103**, 2677–2682.